Chiral two- and three-nucleon interactions used in ring diagram method for binding energy of ^{4}He

Yiharn Tzeng[1], *Shwu-Yun Tsay Tzeng*[2], *T. T. S. Kuo*[3]

[1]Institute of Physics, Academia Sinica, Taipei 11529, Taiwan, ROC
[2]Dept. of Electro-Optical Engineering, National Taipei University of Technology, Taipei 10608, Taiwan, ROC
[3]Department of Physics, State University New York at Stony Brook, New York 11794, USA

In this work, we carry out ring-diagram calculationsfor ^{4}He using the chiral N^{3}LO two-nucleon potential V_{2N} with and without the inclusion of an in-medium three-nucleon (NNN) force $\bar{V}_{3N}$, derived from the leading-order chiral NNN force V_{3N}.

The ring-diagram method [1] is based on the the linked-diagram expansion [2] where the ground-state energy shift ΔE_0 is given by $\Delta E_0 = E_0 - E_0^{\text{free}} = \lim_{t' \to -\infty} \left[\frac{\langle \Phi_0 | V U(0,t') | \Phi_0 \rangle}{\langle \Phi_0 | U(0,t') | \Phi_0 \rangle} \right]_{\text{linked}}$ with $U(0,t')$ the time-evolution operator, and E_0 and E_0^{free} respectively the true and non-interacting ground-state energies of the nuclear system with the nuclear hamiltonian $H = T + V$, Φ_0 the system's unperturbed shell-model ground-state wave function. Here we take $V = V_{2N} + \bar{V}_{3N}$.

In calculating ΔE_0, we include only all-order sum of the *pphh* ring diagrams as illustrated in Fig. 1. As shown, diagrams (b), (c) and (d) are respectively the 1st-, 4th- and 8th-order *pphh* diagrams. It may be noted that our ring-diagram calculation reduces to the usual Hartree-Fock (HF) one if only the first order ring diagram (b) is included. A main purpose of our present work is to study the effect of the particle-hole excitations, which are not included in the HF case, to the binding energies of finite nuclei. Indicated by (a) of the Figure is the mean field single particle (s.p.) propagators where the HF one-bubble insertions are included to all orders.
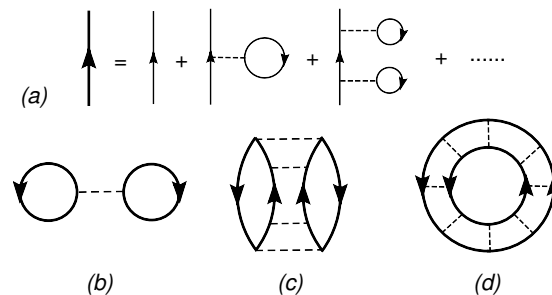
Figure 1: The *pphh* ring-diagrams for the ground state energy shift of closed-shell nuclei; (a) self-energy insertions on the single-particle propagator, and (b) to (d) all-order ring diagrams.

Summing up these ring diagrams to all orders, one has the ground-state energy shift from V as [1]

$$\Delta E_0 = \int_0^1 d\lambda \sum_m \sum_{ijkl \in P} Y_m(ij,\lambda) Y_m^*(kl,\lambda) \times \langle ij|V|kl\rangle, \tag{1}$$

where (i,j,k,l) are each a shell-model s. p. wave function, and P denotes a chosen shell-model space composed of a set of hole (h) and particle (p) orbits.

The amplitudes Y above are calculated from an RPA-type equation, namely

$$\sum_{ef}[(\epsilon_i + \epsilon_j)\delta_{ij,ef} + \lambda(1 - n_i - n_j)\langle ij|V|ef\rangle] \times Y_m(ef,\lambda) = \omega_m(\lambda)Y_m(ij,\lambda); \quad (i,j,e,f) \in P, \tag{2}$$

where λ is a strength parameter, to be integrated from 0 to 1 as in Eq. 2. The occupation factors are $n_a = 1$ for $a = h$, and $= 0$ otherwise. Thus the amplitudes $Y_m(ij)$ has only either hh $(i = h, j = h')$ or pp $(i = p, j = p')$ components. The transition amplitudes Y can be classified into two types, one dominated by hh and the other by pp components. We include only the former, denoted by Y_m, for the calculation of the all-order sum of the $pphh$ ring diagrams.

We use HF s.p. spectrum ϵ_j in the above RPA equation, as indicated earlier in Fig. 1, namely $\epsilon_j = \langle j|K_{sp}|j\rangle + \sum_h \langle jh|V|jh\rangle$ where K_{sp} denotes the s. p. kinetic energy operator. Note that j and h are each oscillator s. p. wave function.

To carry on, we need first describe the V_{3N} to be employed. The leading contribution to V_{3N} occurs at N²LO in the chiral power counting and is composed of a long-range two-pion exchange $V_{3N}^{2\pi}$, a medium-range one-pion exchange $V_{3N}^{1\pi}$, and a pure contact interaction V_{3N}^{ct}:

$$V_{3N}^{(2\pi)} = \sum_{i \neq j \neq k} \frac{g_A^2}{8f_\pi^4} \frac{\vec{\sigma}_i \cdot \vec{q}_i \, \vec{\sigma}_j \cdot \vec{q}_j}{(\vec{q}_i^{\,2} + m_\pi^2)(\vec{q}_j^{\,2} + m_\pi^2)} F_{ijk}^{\alpha\beta} \tau_i^\alpha \tau_j^\beta, \tag{3}$$

$$V_{3N}^{(1\pi)} = -\sum_{i \neq j \neq k} \frac{g_A c_D}{8f_\pi^4 \Lambda_\chi} \frac{\vec{\sigma}_j \cdot \vec{q}_j}{\vec{q}_j^{\,2} + m_\pi^2} \vec{\sigma}_i \cdot \vec{q}_j \, \vec{\tau}_i \cdot \vec{\tau}_j, \qquad V_{3N}^{(ct)} = \sum_{i \neq j \neq k} \frac{c_E}{2f_\pi^4 \Lambda_\chi} \vec{\tau}_i \cdot \vec{\tau}_j, \tag{4}$$

with $g_A = 1.29$, $f_\pi = 92.4$ MeV, $\Lambda_\chi = 700$ MeV, and $m_\pi = 138.04$ MeV/c^2 the average pion mass, $\vec{q}_i = \vec{p_i}' - \vec{p_i}$ is the difference between the final and initial momentum of nucleon i and $F_{ijk}^{\alpha\beta} = \delta^{\alpha\beta} \left(-4c_1 m_\pi^2 + 2c_3 \vec{q}_i \cdot \vec{q}_j\right) + c_4 \epsilon^{\alpha\beta\gamma} \tau_k^\gamma \vec{\sigma}_k \cdot (\vec{q}_i \times \vec{q}_j)$. The low-energy constants $c_1 = -0.76 \, \text{GeV}^{-1}$, $c_3 = -4.78 \, \text{GeV}^{-1}$, and $c_4 = 3.96 \, \text{GeV}^{-1}$ appear already in the N²LO two-nucleon potential and are thus constrained by low-energy NN phase shifts [3]. The constants c_D and c_E are typically fit to reproduce the properties of light nuclei [4, 5].

As mentioned earlier, the interaction $V = (V_{2N} + \bar{V}_{3N})$ will be employed in our calculations. V_{2N} is the NN interaction obtained from a N³LO chiral two-body potential [6] and $\bar{V}_{3N}$ is a density-dependent two-body interaction obtained from the chiral three nucleon force by closing one pair of external lines and summing over the filled Fermi sea (k_F) of nucleons [7]. $\bar{V}_{3N}$ and V_{3N} are related by $\langle ab|\bar{V}_{3N}|cd\rangle = \sum_{h \leq k_F} \langle abh|V_{3N}|cdh\rangle$, where the matrix elements are anti-symmetrized. Possible over-counts are carefully treated. $\bar{V}_{3N}$ is dependent of k_F or its corresponding density n.

We then calculate effective low momentum V_{low-k} matrix elements [8] from V_{2N} and V_{3N} for the use in the ring diagram calculations. Starting from the half-on-shell T-matrix in the

Lippmann-Schwinger equation, one defines the effective low-momentum T-matrix as

$$T_{\text{low}-k}(p',p,p^2) = V_{\text{low}-k}(p',p) + \int_0^\Lambda q^2 dq V_{low-k}(p',q)\frac{T_{low-k}(q,p,p^2)}{p^2 - q^2 + i0^+} \tag{5}$$

where Λ denotes a momentum space cut-off and $(p',p) \leq \Lambda$. The T-matrix in Eq.(5) is required to satisfy the condition $T(p',p,p^2) = T_{low-k}(p',p,p^2)$; $(p',p) \leq \Lambda$. Earlier studies shew nuclear properties obtained from V_{low-k} being rather insensitive on Λ in the vicinity of 2.1 fm^{-1} [8]. Hence we set the cut-off in Eq. (5) $\Lambda \approx 2.1$ fm^{-1}.

To calculate the V_{low-k} matrix with V_{3N} included, we have used the Bertsch formula $\hbar\omega = 45.0A^{-1/3} - 25.0A^{-2/3}$. we adopt the magnitudes of parameters c_D, c_E in Eqs. (4) from the c_E vs. c_D curve in [5] where the authors determined values of these two parameters from fitting binding energies of $A = 3$ nuclei. The nucleon density arising from the contact term [7] of Eq. (4) for the nucleus is chosen from the experimental charge density profile $\rho(r)$ vs. r from [9] as that approximately at the nucleus' RMS radius. The RMS radius for ^{4}He is 1.6757 fm [10] In this way, we set the density around the RMS radius to be $0.3\rho_0$ for ^{4}He, with $\rho_0 = 0.17$/fm^3.

The empirical Coulomb energy $E_{coul}/A = 0.717 \times Z^2/A^{4/3}$ is added to the nuclear system's ground state energy. Note that the non-interaction ground state energy E_0^{free} already takes care of the center of mass motion part. Hence our ring diagram expansion of ΔE_0 involves no CM excitation problems.

Shown in Fig. 2 is the dependence of ground state energy per nucleon (or -BE/A) for ^{4}He on the 3N force constant c_D appearing in Eq. (4). In the figure, results from the first order ring diagram ("HF"), up to the second order one("Up to 2nd"), and all order ring diagrams ("Ring(all)") are all calculated with V_{3N} included. Experimental data [11] are displayed for comparison. Although the contribution from diagrams up to the second order one improves quite significantly comparing to that from the first order one alone, contribution from higher order diagrams is needed to fill the discrepancy so that the experimental binding energy can be obtained.
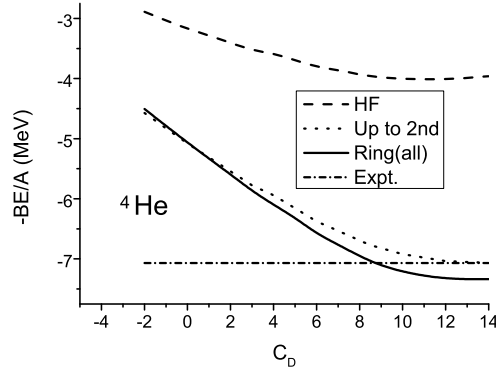
Figure 2: Dependence of $-BE/A$ of ^{4}He on the parameter c_D of V_{3N}.

As shown in Table I, our results from $V_{2N} + \bar{V}_{3N}$ with parameter c_D= 8.5 and its corresponding c_E from [5] at density ρ/ρ_0= 0.3 for ^{4}He fits the experimental data [11] quite well. In

the Table we also examine the importance of V_{3N} to the nuclear binding energy. As expected, the binding energy obtained from V_{2N} alone is too weak. The deviation between results with and without V_{3N} gets wider when all ring diagrams are included.

Table 1: Ground-state energy E_0/A (or -BE/A)(in MeV) of ^{4}He calculated with 1st-, (1st+2nd)- and all-order ring diagrams. The parameter $c_D = 8.5$ of $\bar{V}_{3N}$ is employed.

		ρ/ρ_0	1st	1st+2nd	all rings	Expt
^{4}He	V_{2N}	–	-3.46	-5.36	-5.39	
	$V_{2N}+\bar{V}_{3N}$	0.3	-3.96	-6.77	-7.05	-7.073

In conclusion, our calculated ground state energy per nucleon fits the experimental data quite well when V_{3N} is added in and all orders of ring diagrams are included. Contributions from ring diagrams with orders higher than 2 can not be ignored. As expected, binding energy obtained with V_{2N} alone is too weak. This study shows that the three-nucleon force is important in nuclear systems. We have found that the above results are also true for several other closed-shell nuclei. This will appear in other separate publications.

References

[1] H. Q. Song, S. D. Yang and T.T.S. Kuo, Nucl. Phys. **A462**, 491 (1987); Yiharn Tzeng, T. T. S. Kuo,Nucl. Phys. A485, 85 (1988).

[2] T. T. S. Kuo and E. Osnes, *Lecture Notes in Physics* (Springer-Verlag, New York), Vol. 364 (1990) p.1.

[3] M. C. M. Rentmeester, R. G. E. Timmermans, and J. J. de Swart, Phys. Rev. C **67** (2003) 044001.

[4] A. Nogga, H. Kamada and W. Glockle, Phys. Rev. Lett. **94**, 944 (2000); S.C. Peiper, K. Varga and R. B. Waringa, Phys. Rev. **C66**, 044310 (2002).

[5] P. Navratil, V.G. Gueorguiev, J.P. Vary, W.E. Ormand and A. Nogga, Phys. Rev. Lett. **99**, 042501 (2007).

[6] D. R. Entem, R. Machleidt, and H. Witala, Phys. Rev. C **65**, 064005 (2002).

[7] J. W. Holt, N. Kaiser and W. Weise, Phys. Rev. **C79**, 054331 (2009); J. W. Holt, N. Kaiser and W. Weise, Phys. Rev. **C81**, 024002 (2010).

[8] S. K. Bogner, T. T. S. Kuo and L. Coraggio, Nucl. Phys. **A684**, (2001) 432; S. K. Bogner, T. T. S. Kuo, L. Coraggio, A. Covello, and N. Itaco, Phys. Rev. C **65**, 051301(R) (2002); S. K. Bogner, T. T. S. Kuo, and A. Schwenk, Phys. Rep. **386**, 1 (2003).

[9] J.S.Mccarthy, I. Sick, and R.R. Whitney, Phys. Rev. C **15**, 1396 (1977); H. de Vries, C.W. de Jager, and C. de Vries, At. Data Nucl. data Tables, **36**, 495 (1987)

[10] I. Angeli, K.P. Marinova, Atomic and Nucl. Data Tables **99** 69 (2013).

[11] B.Pfeiffer,K.Venkataramaniaih,U.Czok,C.Scheidenberger, Atomic and Nucl. Data Tables **100** 403-535 (2014); Nuclear data from Brookhaven National Laboratory, http://www.nndc.bnl.gov/chart/